

# Fabrication of Porous Si@C Composites with Core-Shell Structure and Their Electrochemical Performance for Li-ion Batteries

Shuo Zhao <sup>1,\*</sup>, Yue Xu <sup>1</sup>, Xiaochao Xian<sup>1,\*</sup>, Na Liu <sup>2,3</sup>, Wenjing Li <sup>4</sup>

<sup>1</sup> School of Chemistry and Chemical Engineering, Chongqing University, Chongqing 400030, PR China; 17754925865@163.com

<sup>2</sup> Department of Chemistry, Hengshui University, HeBei 053000, PR China; ln281828541@hotmail.com

<sup>3</sup> Department of Pharmaceutical and Cosmetical Engineering, Woosuk University, Jeollabuk-do, 55338, Korea

<sup>4</sup> National Oil Reserve Center, Beijing 100000, PR China; cqzs@163.com

\* Correspondence: zhaoshuo@cqu.edu.cn (S.Z.); xiaochx@cqu.edu.cn (X.X.)

Received: 17 January 2019; Accepted: 25 February 2019; Published: 27 February 2019

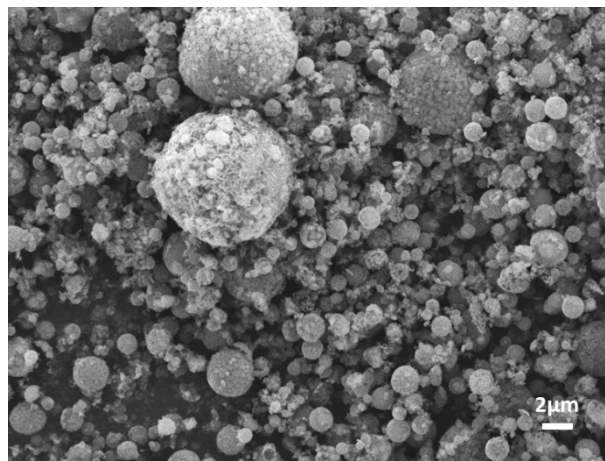
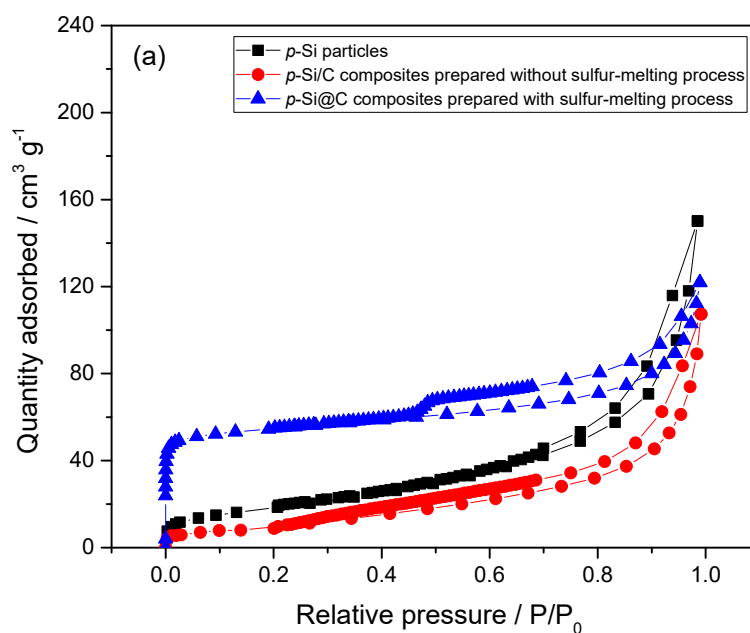
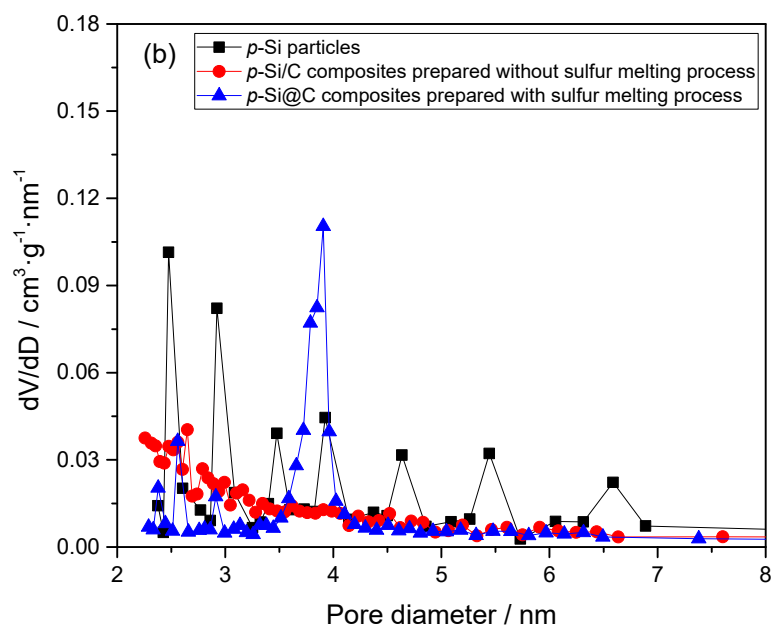


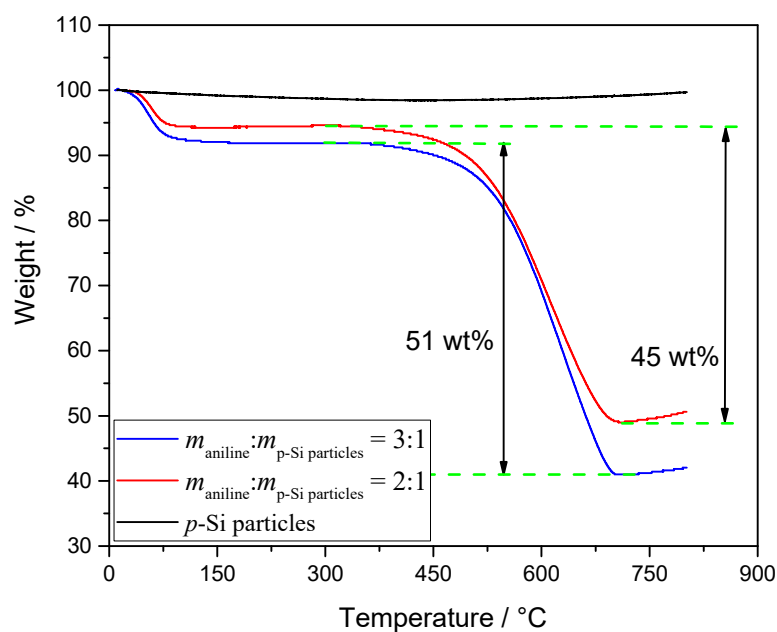
Figure S1. SEM image of Al-Si alloy power.





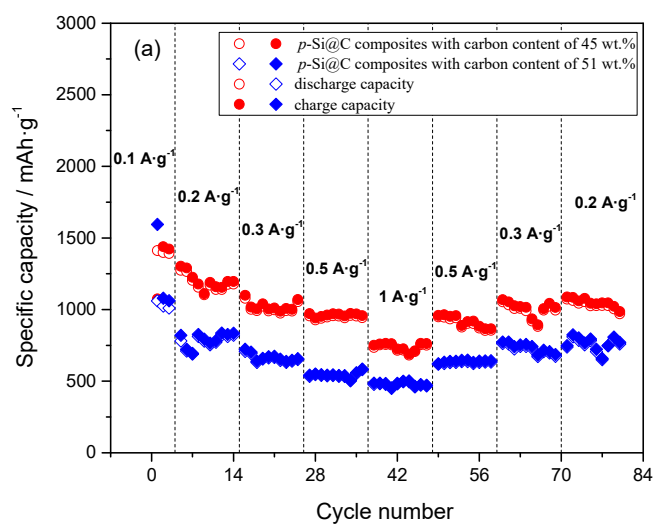
**Figure S2.** (a)  $N_2$  adsorption-desorption isotherms and (b) pore size distribution of *p*-Si particles, *p*-Si/C particles and *p*-Si@C particles.

JW-BK200C Apparatus was used to evaluate the surface areas and porous structure of *p*-Si particles, *p*-Si/C composites prepared without sulfur-melting process and *p*-Si@C composites with sulfur-melting process, and the results are shown in Fig. S2. The results indicate that the curves of *p*-Si particles and *p*-Si/C composites both exhibit H3 hysteresis loops which is typical of slit-shaped pores or the space between different parallel Si particles based on the BDDT classification [1]. As shown in Fig. S2b, the pores with size distribution between 3.5 nm and 7 nm in *p*-Si particles disappear, after coated by PANI-based carbon without sulfur-melting process, moreover, no obvious peaks is observed below 3.5 nm. The results indicates that some pores in *p*-Si particles are occupied by PANI-based carbon during the preparation of *p*-Si/C composites. Therefore, the surface areas of *p*-Si/C composites ( $33 \text{ m}^2\cdot\text{g}^{-1}$ ) is smaller than that of *p*-Si particles ( $62 \text{ m}^2\cdot\text{g}^{-1}$ ). On the other hand, *p*-Si@C composites displays type I isotherm within the range of lower relative pressure ( $P/P_0 = 0\sim 0.01$ ) and type IV isotherm within the range of higher relative pressure ( $P/P_0 > 0.4$ ). Combining the results in Fig. S2, it can be concluded that the pores in *p*-Si particles are retained and the outer carbon layer is porous in *p*-Si@C composites. Therefore, *p*-Si@C composites have high surface areas ( $207 \text{ m}^2\cdot\text{g}^{-1}$ ).



**Figure S3.** TGA curves of *p*-Si particles and *p*-Si@C composites obtained from different mass ratios of aniline and porous silicon particles.

Carbon contents in *p*-Si@C composites were estimated under air by thermogravimetric analysis (TGA) on TGA/DSC simultaneous thermal analyzer (Mettler Toledo TGA/DSC/1600LF, Switzerland). The carbon contents of *p*-Si@C composites prepared from  $m_{\text{aniline}} : m_{p\text{-Si particles}} = 2:1$  and  $3:1$  are about 45 wt.% and 51 wt.%, respectively.



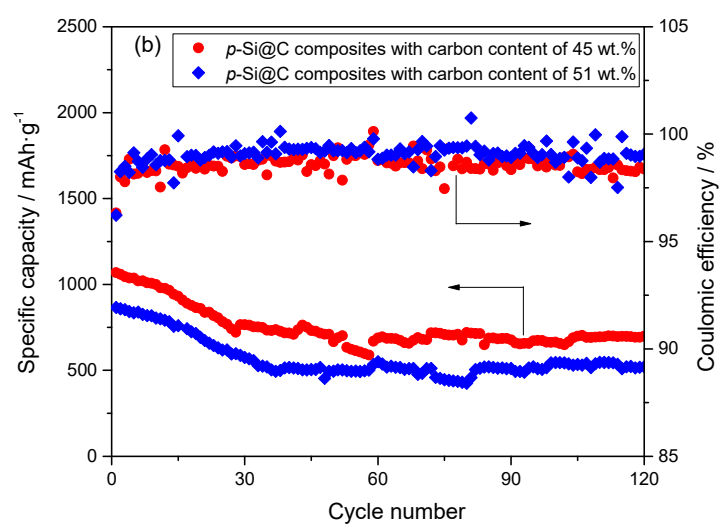


Figure S4. performance for *p*-Si@C composites with different carbon contents.

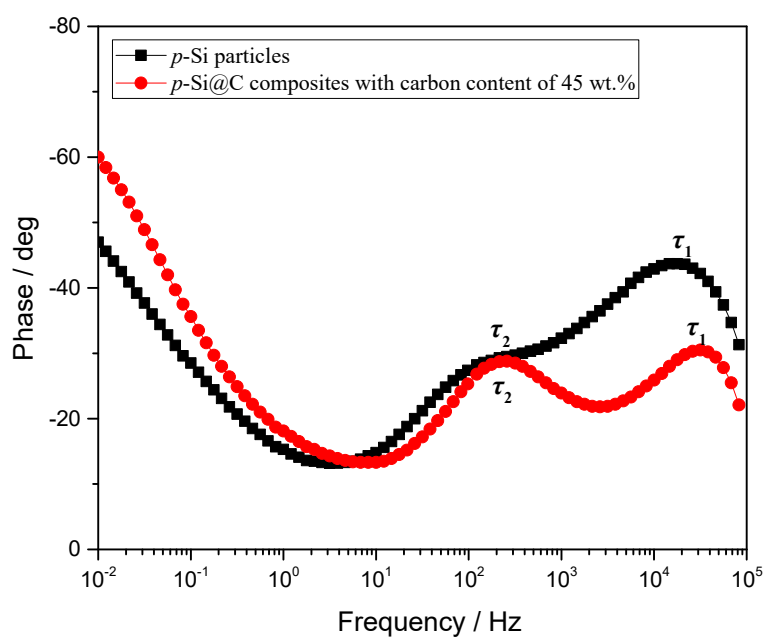


Figure S5. Bode plots for *p*-Si particles and *p*-Si@C composites with carbon contents of 45 wt. %.

## Reference

1. Pan, C.; Zhang, D.; Shi, L. CTAB assisted hydrothermal synthesis, controlled conversion and CO oxidation properties of CeO<sub>2</sub> nanoplates, nanotubes, and nanorods. *J. Solid State Chem.* **2008**, *181*, 1298-1306.